

## Pt magnetization profile in a Pt/Co bilayer studied by resonant magnetic x-ray reflectometry

J. Geissler, E. Goering, M. Justen, F. Weigand, and G. Schütz  
*Universität Würzburg, Experimentalphysik IV, Am Hubland, D-97074 Würzburg, Germany*

J. Langer, D. Schmitz, and H. Maletta  
*Hahn-Meitner-Institut Berlin, Glienicker Strasse 100, D-14109 Berlin, Germany*

R. Mattheis  
*Institut für Physikalische Hochtechnologie, Winzerlaer Strasse 10, D-07745 Jena, Germany*  
 (Received 11 October 2001; published 13 December 2001)

The Pt magnetization depth profile at a single buried Pt/Co interface was investigated by x-ray resonant magnetic reflectivity measurements. The asymmetry as function of angle of incidence has been measured in the Pt  $L_3$ -near-edge absorption region at two energies. Observed asymmetry ratios in the order of 0.5% are described on the basis of a magnetically modified Parratt algorithm. Excellent agreement between simulations and experiment was achieved for a Pt magnetic moment of  $0.21\mu_B$  at the rough interface followed by an exponential decay of the induced polarization within 1 nm.

DOI: 10.1103/PhysRevB.65.020405

PACS number(s): 75.70.Cn, 78.70.Ck, 75.50.Ss, 83.85.Hf

Multilayered systems consisting of magnetic and nonmagnetic components have gained steadily growing interest from fundamental physical aspects as well as for technical applications, since these artificial media exhibit new fascinating properties. Due to the oscillatory exchange coupling in combination with giant magnetoresistance (GMR)<sup>1</sup> and tunnel magnetoresistance (TMR)<sup>2</sup> they work as basic components for magnetic sensors and magneto- and spin-electronic devices as used in magnetic random access memories (MRAM's). Furthermore, the presence of interfaces can cause a perpendicular magnetic anisotropy which is an advantage for high density hard disk media and required for magneto-optical recording. In this field Pt/Co systems play a dominant role. Hysteresis characteristics, easily adjustable by the choice of composition, long stability against corrosion and the significant increase of the Kerr rotation in the blue laser regime<sup>3</sup> are some of the appealing aspects for technical applications. Platinum is crucial for the magnetism of these systems, since the late  $d$ -transition elements can be significantly magnetically polarized in the vicinity of ferromagnetically ordered atoms due to the large Stoner factor.

Magnetic properties of artificial multilayered media are strongly influenced by growth preparation conditions, subsequent thermal treatment, and hydrogen charging.<sup>4</sup> Hereby the morphology of the interface and particularly its roughness plays the major role for global electronic, magnetic, transport, and optical properties.<sup>5</sup> The reliable determination of lateral and perpendicular interface characteristics is crucial for further developments in material science.

In most of the technical relevant systems these interfaces are buried underneath several nanometers. Methods with atomic resolution as STM, atomic force microscopy (AFM) and the magnetic counterparts spin-polarized STM and MFM are restricted to surfaces. Polarized neutron reflectometry<sup>6</sup> as a complementary method cannot simply distinguish between induced and interdiffused magnetization of different components.

Due to strongly enhanced magnetic contributions in the resonant scattering cross section, it is possible to study also in an element and site-selective manner magnetic characteristics of structural components by x-ray resonant magnetic scattering (XRMS) of polarized synchrotron radiation in the hard and soft x-ray range.<sup>7,8</sup> Under Bragg conditions XRMS is also surface sensitive by measuring truncation rods under grazing incidence.<sup>9,10</sup> Superlattice reflections in multilayers contain information of layer-averaged properties, for, e.g., magnetization depth profiles, of one component of the whole multilayer system.<sup>11-13</sup> Thus lateral variations and their dependence of the distance of an individual layer from the substrate, important for components with large lattice mismatch, can hardly be addressed. Furthermore, diffuse XRMS in the soft x-ray region can be applied to investigate correlations between chemical and magnetic roughness in thin films and multilayers.<sup>14,15</sup>

In this paper we demonstrate that magnetic resonant reflectivity measurements in the hard x-ray range give detailed element-specific quantitative insight into the magnetization profile at a single buried interface. Comparable to nonmagnetic specular reflectivity experiments, which yield to well known analysis of layer thickness and interface roughness, specular magnetic measurements provide quantitative information of magnetization profiles perpendicular to the surface due to momentum transfer in this direction. Studies were performed on a Pt/Co bilayer using hard x rays in the vicinity of the Pt  $L_3$  edge at the energy of the maximum amplitude of the effect of x-ray magnetic circular dichroism (XMCD). To verify the extracted Pt magnetization profile, a second magnetic reflectivity profile was taken at the low energy side of the Pt white line, where the maximum magnetic scattering amplitude occurs and the absorption is significantly reduced. We evaluated the depth profile of the Pt magnetization by a magnetically modified Parratt algorithm<sup>16</sup> regarding magnetical resonant induced changes of the scattering form factor.<sup>18</sup>

The Pt 6.2 nm/Co 2.6 nm/Cu 2.5 nm/Ta 4.3 nm/Si-substrate thin film was prepared by dc-sputter deposition in a

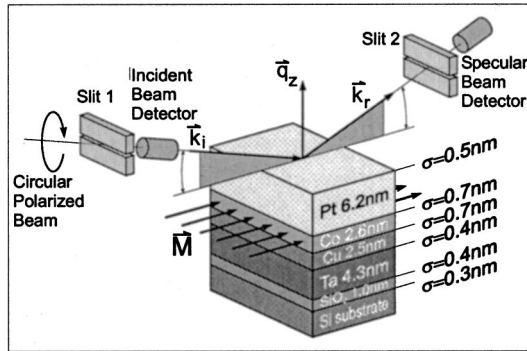


FIG. 1. Schematic experimental setup, layer thicknesses, and rms roughnesses of the sample determined by nonresonant Cu  $K\alpha$  reflection.

conventional vacuum system on a Si (111). The size of the sample was about  $50 \times 16 \text{ nm}^2$ . To reduce the number of free parameters, thickness and interfacial roughness of the sample were separately determined with Cu  $K\alpha$  reflectometry<sup>17,18</sup> and simulated with the HMI code.<sup>19</sup> SQUID measurements showed an in-plane easy axis with 20 Oe remanence field.

The actual composition and interfacial roughness for each layer and the setup of the magnetic reflectivity experiment in  $\theta$ - $2\theta$  geometry are shown in Fig. 1. Measurements were performed at HASYLAB/Germany at beamlines A1 and BW4. A degree of circular polarization of  $P_C=0.54$  was achieved at the Wiggler beamline BW4 utilizing a diamond phase retarder. At the bending magnet beamline A1 circular polarized light with  $P_C=0.8$  was used. The degree of magnetization at room temperature was 0.82 relative to  $T=0 \text{ K}$ . The incoming and reflected intensities were detected by ionization chambers.

To adjust to the energy where the absorptive and dispersive part of the magnetic scattering amplitudes  $m'(E)$  and  $m''(E)$  are at maximum the Pt  $L_3$  absorption profile  $\mu(E)$  and the corresponding XMCD  $\mu_C(E) = (\mu^+ - \mu^-)/2$  have been measured in a separate transmission experiment on a sequence of XPt/0.4 nm Co multilayers. It has been proven that for Pt thicknesses more than  $X=0.9 \text{ nm}$  only the amplitude of  $\mu_C(E)$  decreases, while its profile stays identical.<sup>20</sup> The optical theorem relates the absorptive scattering amplitude  $f''$  to the absorption coefficient  $\mu(E)$ , while the absorptive contribution to the magnetic scattering amplitude is  $m'' = \mu_C(E)/\mu(E) \cdot f''$  and the time-even part  $f'$  and time-odd part  $m'$  of the optical constant are deduced by a Kramers-Kronig relation.<sup>21,22</sup> The absorption profile and the energy dependence of the magnetic scattering amplitudes are presented in Fig. 2, determining the energy values of maximum  $m''$  ( $E_1=11566 \text{ eV}$ ) and the minimum of  $m'$  ( $E_2=11562 \text{ eV}$ ).

The reflectivity at these energies was measured in a  $\theta$  range from 0.001 to 1.1 deg in steps of 0.002 deg and the asymmetry was obtained by flipping the sample magnetization parallel and antiparallel to the direction of the incoming photon beam at each angle position. The reflectivity and the obtained asymmetry ratios  $A = (I^+ - I^-)/(I^+ + I^-)$  for both energies  $E_1$  and  $E_2$  are shown in Fig. 3.

For a theoretical description of these experimental find-

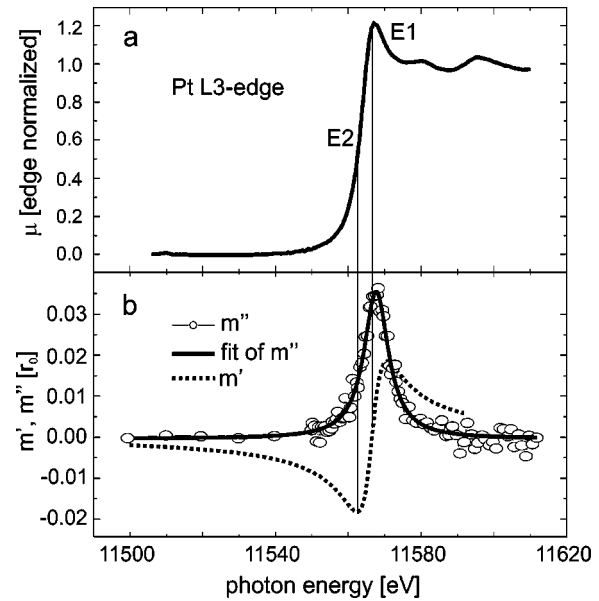


FIG. 2. (a) Edge normalized Pt  $L_3$  absorption profile of a 2.3 nm Pt/0.4 nm Co multilayer. (b) Absorptive magnetic Pt scattering amplitude  $m''$  (circles) deduced from the Pt- $L_3$  XMCD spectra and its Lorentzian fitted representation (solid line). Dispersive part  $m'$  (dotted line) derived by Kramers-Kronig relation from the fitted  $m''$ . Maximum amplitudes of  $m''$  and  $m'$  at two different energies  $E_1$  and  $E_2$  are marked by vertical thin lines.

ings one has to consider that the specular reflected intensity of x rays depends both on the real and imaginary part of the index of refraction  $n = 1 - \delta - i\beta$  with the optical constants  $\delta$  and  $\beta$ , which are related to the real and imaginary part of the scattering amplitude  $f'$  and  $f''$ . In dipole approximation the resonant x-ray atomic form factor of a magnetic atom is<sup>8</sup>

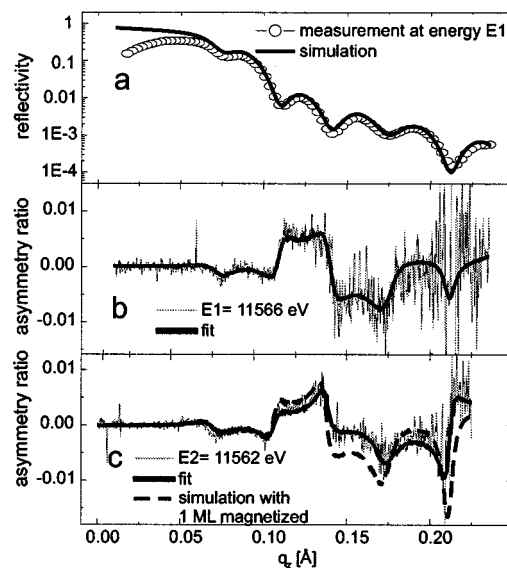


FIG. 3. Reflected intensity (a) and asymmetry ratios (light lines) normalized to the degree of circular polarization at energies  $E_1 = 11566.2 \text{ eV}$  (b) and  $E_2 = 11562.2 \text{ eV}$  (c) compared to simulations (dark lines). The calculated asymmetry curve (c) for a Pt polarization concentrated in the first monolayer carrying the same total magnetization (dashed line).

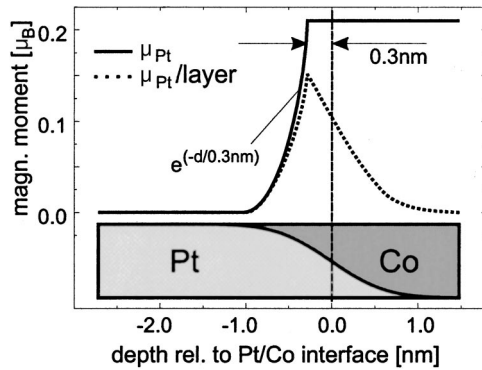


FIG. 4. Profile of the induced Pt 5d magnetic polarization per Pt atom (straight line) and per layer (dotted). In addition the chemical profile of the Pt/Co interface is shown at the bottom.

$$f(E, \theta) = -(\mathbf{e}_f \cdot \mathbf{e}_i)[f_0(\theta) + f'(E) + if''(E)] - i(\mathbf{e}_f \times \mathbf{e}_i) \mathbf{z}[m'(E) - im''(E)]. \quad (1)$$

$E$  is the photon energy,  $\mathbf{e}_i$  and  $\mathbf{e}_f$  are the polarization vectors of the incident and scattered beam,  $\mathbf{z}$  is the unit vector of the magnetization, and  $f_0(\theta)$  is the conventional atomic form factor. For the small angles of incident used in the experiment it is sufficient to consider only forward scattering processes and the magnetic term contributes additively to the nonmagnetic scattering amplitudes reduced by the degree of circular polarization  $P_C$  and due to the finite degree of magnetization  $M(T)/M(0)$ .

For a structure consisting of a sequence of layered media with different indices of refraction separated by rough interfaces the evaluation of the resulting reflection amplitude leads to a recursive equation first carried out by Parratt<sup>16</sup>

$$R_i = \frac{R_{t,i} + R_{b,i} \exp(2i\varphi)}{1 + R_{t,i} R_{b,i} \exp(2i\varphi)}. \quad (2)$$

Here  $R_{t,i}$  and  $R_{b,i}$  are the Fresnel reflection amplitudes at the top and bottom surface of the layer  $i$ , modified by a statistical “Debye-Waller” factor taking into account the attenuation due to the mean vertical roughness, described by the value  $\sigma$  (RMS roughness) as suggested by Névot and Croce.<sup>23</sup> The phase difference  $\varphi_i = 2\pi/\lambda d_i n_i \sin \alpha_i$  is related to the thickness  $d_i$  of the layer illustrating the depth sensitivity of specular reflectometry. This method takes into account all scattered light intensities and phases inside the multilayer structure interactively, which is necessary for a high qualitative and quantitative description of experimental data. For magnetic simulations chemical thickness and roughness values from the nonmagnetic Cu  $K\alpha$  reflectivity were used and the asymmetry was deduced from simulated reflectivities  $I^+$  and  $I^-$ . The chemical (optical) density profile shown in the lower part of Fig. 4 of the Pt/Co interface was modeled by a set of thin layers of 0.1 nm thickness with optical constants  $n_{\text{chem}}(z)$ , which is an equivalent description for rough interfaces to the above described RMS roughness  $\sigma$ . The anomalous resonant scattering amplitudes  $f'$  and  $f''$  of Pt were determined as described above and tabulated val-

ues have been used for other elements.<sup>24</sup> The free parameter in simulations is the change of the optical constants  $n_{\text{mag}}(z)$  of each modeled layer due to the magnetization of each Pt atom (Fig. 4, straight line), given by  $m'$  and  $m''$ . The corresponding magnetization of each modeled thin layer

$$n_m(z) = n_{\text{chem}}(z) + n_{\text{mag}}(z) = p(z)[n_{\text{Pt}}^0 + n_{\text{Pt}}^{\text{mag}}(z)] + [p(z) - 1][n_{\text{Co}}^0] \quad (3)$$

originated from the Pt polarization is the convolution of the Pt concentration  $p(z)$  and the magnetization per Pt atom and shown by the dotted line in Fig. 4. Simulations of  $n_{\text{Pt}}^{\text{mag}}(z)$  were done for a large set of different length parameters and magnetization decay profiles. Therefore a clear exponential decay and an upper limit of 0.1 nm length scale error can be deduced. The simulation technique represents a modeling of a density gradient. The strong dependence of the reflectivity coefficient on density gradients results in the high length scale resolution and the strong sensitivity of the simulated asymmetry ratios.

The simulation of the reflectivity and the asymmetry ratios for both energies are presented in Fig. 3. Excellent agreement with measured asymmetries was obtained by a constant magnetization per Pt atom of  $(0.21 \pm 0.04)\mu_B$  up to  $(0.3 \pm 0.1)$  nm (1 ML) above the point of inflection of the chemical profile (Fig. 4, bottom) followed by an exponential decay with a decay length of  $(0.3 \pm 0.1)$  nm. To illustrate the sensitivity to the magnetic depth profile the asymmetry expected for the same total Pt magnetization artificially localized in 1 ML at the point of inflection is included in Fig. 3(c) (dashed line) which show a strongly different behavior pronounced at larger reflection angles. We want to point out that the evaluated Pt magnetization profile depends on the chemical profile and is therefore not unique for Pt/Co interfaces with different chemical density gradients.

Absolute values of magnetic moments per Pt atom were obtained from the local ratio  $m''/f''$  with the normalized integral dichroism amplitude  $\mu_c/\mu_0$  from measurements reported in Refs. 20, 25 and 26 taking into account the degree of circular polarization and the reduced magnetization of the sample. These results are in good agreement with Pt XMCD results of XPt/2Co multilayer systems.<sup>20,26</sup>

In conclusion we have determined quantitatively the profile of the induced magnetic 5d moment of Pt at a single Pt/Co interface. In contrast to XRMS at superlattice Bragg peaks it is possible to determine the magnetization of a single layer. Compared to complementary techniques as measuring magnetic truncation rods this method is not restricted to media with well defined crystalline structures. The magnetization profile was deduced from the measured asymmetry ratio in the resonant reflectivity and modeling with a magnetically modified Parratt formalism. Absolute values of the magnetization were determined by scaling  $m''/f''$  to the normalized dichroism amplitude from previous XMCD absorption measurements of Pt/Co multilayer. It is demon-

strated that high sensitivity can be gained for all relevant sublayers even for small induced magnetic moments. A clear separation of chemical and magnetic profiles (vertical roughness) has been performed. In the future this method allows studies of the interplay between chemical magnetic roughness of single layers. Hereby one interesting application of the presented method is the new possibility for quantitative and site-selective studies of magnetic depth profiles in GMR

systems, magnetic tunneling junctions, MRAM's, or other future magnetic thin film spin electronic devices.

We thank A. Bauer (Friedrich-Schiller-University Jena) for characterizing the Si substrate, K. Attenkofer and G. V. Krosigk (HASYLAB) for assistance with the XMCD measurements, and W. Michalke (IPHT Jena) for the sample preparation.

- 
- <sup>1</sup>G. Binasch, P. Grünberg, F. Saurenbach, and W. Zinn, *Phys. Rev. B* **39**, 4828 (1989).
- <sup>2</sup>J. S. Moodera, L. R. Kinder, T. M. Wong, and R. Meservey, *Phys. Rev. Lett.* **74**, 3273 (1995).
- <sup>3</sup>W. P. Zeper, F. J. A. M. Greidanus, P. F. Garcia, and C. R. Fincher, *J. Appl. Phys.* **65**, 4971 (1989).
- <sup>4</sup>F. Klose, Ch. Rehm, D. Nagengast, H. Maletta, and A. Weidinger, *Phys. Rev. Lett.* **78**, 1150 (1997).
- <sup>5</sup>P. Bruno, *Phys. Rev. B* **52**, 411 (1995).
- <sup>6</sup>T. Nawrath, H. Fritzsche, F. Klose, J. Nowikow, and H. Maletta, *Phys. Rev. B* **60**, 9525 (1999).
- <sup>7</sup>D. Gibbs, D. R. Harshman, E. D. Isaacs, D. B. McWhan, D. Mills, and C. Vettier, *Phys. Rev. Lett.* **61**, 1241 (1988).
- <sup>8</sup>J. P. Hannon, G. T. Trammell, M. Blume, and D. Gibbs, *Phys. Rev. Lett.* **61**, 1245 (1988).
- <sup>9</sup>S. Ferrer, J. Alvarez, E. Lundgren, X. Torrelles, P. Fajardo, and F. Boscherini, *Phys. Rev. B* **56**, 9848 (1997).
- <sup>10</sup>J. Alvarez, E. Lundgren, X. Torrelles, H. Isern, K. F. Peters, P. Steadman, and S. Ferrer, *Phys. Rev. B* **60**, 10 193 (1999).
- <sup>11</sup>J. M. Tonnerre, L. Seve, D. Raoux, G. Soullie, B. Rodmacq, and P. Wolfers, *Phys. Rev. Lett.* **75**, 740 (1995).
- <sup>12</sup>L. Seve, N. Jaouen, J. M. Tonnerre, D. Raoux, F. Bartolome, M. Arend, W. Felsch, A. Rogalev, J. Goulon, C. Gautier, and J. F. Berar, *Phys. Rev. B* **60**, 9662 (1999).
- <sup>13</sup>N. Jaouen, J. M. Tonnerre, E. Bontempi, D. Raoux, L. Seve, F. Bartolome, A. Rogalev, M. Müenzenberg, W. Felsch, H. A. Dürr, E. Dudzik, and H. Maruyama, *Physica B* **283**, 175 (2000).
- <sup>14</sup>J. F. MacKay, C. Teichert, D. E. Savage, and M. G. Lagally, *Phys. Rev. Lett.* **77**, 3925 (1996).
- <sup>15</sup>R. M. Osgood III, S. K. Sinha, J. W. Freeland, Y. A. Idzerda, and S. D. Bader, *J. Appl. Phys.* **85**, 4619 (1999).
- <sup>16</sup>L. G. Parratt, *Phys. Rev.* **95**, 359 (1954).
- <sup>17</sup>S. K. Sinha, E. B. Sirota, S. Garoff, and H. B. Stanley, *Phys. Rev. B* **38**, 2297 (1988).
- <sup>18</sup>V. Holy, J. Kubena, I. Ohlidal, K. Lischka, and W. Plotz, *Phys. Rev. B* **47**, 15 896 (1993).
- <sup>19</sup>Parratt32 code distributed by HMI Berlin.
- <sup>20</sup>S. Rüegg, G. Schütz, P. Fischer, R. Wienke, W. B. Zeper, and H. Ebert, *J. Appl. Phys.* **69**, 5655 (1991).
- <sup>21</sup>J. J. Hoyt and D. de Fontane, *J. Appl. Crystallogr.* **17**, 344 (1984).
- <sup>22</sup>C. Neumann, A. Rogalev, J. Goulon, M. Lingham, and E. Ziegler, *J. Synchrotron Radiat.* **5**, 998 (1998).
- <sup>23</sup>L. Nénot and P. Croce, *J. Phys. Chem.* **15**, 761 (1980).
- <sup>24</sup>C. T. Chantler, *J. Phys. Chem. Ref. Data Monogr.* **24**, 71 (1995).
- <sup>25</sup>G. Schütz, R. Wienke, W. Wilhelm, W. Wagner, P. Kienle, R. Zeller, and R. Frahm, *Z. Phys. B: Condens. Matter* **75**, 495 (1989).
- <sup>26</sup>G. Schütz, H. Ebert, P. Fischer, S. Rüegg, and W. B. Zeper, in *Magnetic Surfaces, Thin Films, and Multilayers*, edited by S. S. P. Parkin, H. Hopster, J.-P. Renard, T. Shinjo, W. Zinn, Mater. Res. Soc. Symp. Proc. No. 231 (Materials Research Society, Pittsburgh, 1991).